

Shot noise in magnetic tunnel junctions from first principles

Kai Liu and Ke Xia

Department of Physics, Beijing Normal University, Beijing 100875, China

Gerrit E. W. Bauer

*Institute for Materials Research, Tohoku University, Sendai 980-8577, Japan and
Kavli Institute of NanoScience, Delft University of Technology, 2628 CJ Delft, The Netherlands*

(Dated: September 29, 2018)

We compute the shot noise in ballistic and disordered Fe|MgO|Fe tunnel junctions by a wave function-matching method. For tunnel barriers with $\lesssim 5$ atomic layers we find a suppression of the Fano factor as a function of the magnetic configuration. For thicker MgO barriers the shot noise is suppressed up to a threshold bias indicating the onset of resonant tunneling. We find excellent agreement with recent experiments when interface disorder is taken into account

PACS numbers: 72.25.Ba, 85.75.-d, 72.10.Bg

The statistics of electron transport in mesoscopic systems has been subject to intensive research in the last decades leading to important and useful insights [1, 2]. In a two-terminal conductor with a time-dependent current $I(t)$, the simplest measure is the noise power $P(\omega) = \int_{-\infty}^{\infty} \langle \Delta I(0) \Delta I(t) \rangle e^{i\omega t} dt$, where $\Delta I(t) \equiv I(t) - \langle I \rangle$ denote the instantaneous fluctuation from the average current and $\langle \dots \rangle$ a time and statistical average. The shot noise S is the zero frequency limit of the noise power when the applied voltage $|eV|$ is sufficiently larger than the thermal energy $k_B T$. The classical shot noise characterized by an uncorrelated Poissonian process is given by the Schottky formula $S = 2e\langle I \rangle$ [3]. Shot noise contains information about the charge of the elementary excitations, entanglement, wave *vs.* particle nature of electron transport, and provides a diagnostic for open transport channels [4].

Magnetic tunnel junctions (MTJs) with MgO barriers [5, 6] have great potential for applications in magnetic random access memory elements and high-frequency generators [7–10]. Band structure calculations of isomorphic Fe|MgO|Fe layered structures predicted a large drop in the electric resistance when the relative magnetization direction of the two ferromagnets switches from antiparallel to parallel [11, 12]. The subsequently observed large tunnel magnetoresistance (TMR) [5, 6] can be explained in terms of the symmetry matching of only the majority-spin states in Fe with the Δ_1 -band of MgO, which is the by far least evanescent in the gap. The tunneling ratio of the majority spin electrons is therefore relatively high while minority spin states are efficiently filtered out by the MgO barrier. However, a quantitative first-principles description of transport in magnetic tunneling junctions is complicated by defects. The chemical composition of the interface strongly affects the TMR [13–15] and various interfacial defects have been identified to reduce the TMR [16–18]. The I-V curves alone cannot discriminate between the possible different origins that reduce the TMR.

According to conventional wisdom shot noise in tun-

nel junctions is classical [1], in agreement with earlier experiments [19, 20]. Recent evidence that shot noise in MTJs is suppressed in the parallel configuration came as a big surprise [21]. In order to resolve this issue we present parameter-free calculations of shot noise in magnetic tunnel junctions. We compute sub-Poissonian shot noise for the parallel magnetic configuration and explain the results in terms of highly-transmitting resonant tunneling between states localized at the interfaces between the ferromagnet and insulator. The agreement between first-principles theory and experiments [21] is quantitative when disorder is taken into account. These results provide strong evidence of coherent transport and (additional) proof for the very high quality of the MTJs used in that study.

According to the scattering theory of transport a two-terminal conductor subjected to a sufficiently small bias voltage V leads to a time-averaged electric current

$$\langle I \rangle = \frac{e^2}{h} |eV| \text{Tr}(\mathbf{t}^\dagger \mathbf{t}) \quad (1)$$

and shot noise

$$S = \frac{2e^2}{h} |eV| \text{Tr}(\mathbf{r}^\dagger \mathbf{r} \mathbf{t}^\dagger \mathbf{t}) \quad (2)$$

where \mathbf{t} and \mathbf{r} are the matrices of the transmission and reflection coefficients in the space of the transport channels of the leads to the scattering region. These equations become more transparent by making use of the distribution function $\rho(T) = \sum_n \delta(T - T_n)$ of the eigenvalues $\{T_n\}$ of the transmission matrix $\mathbf{T} = \mathbf{t}^\dagger \mathbf{t}$, where $T_n \in [0, 1]$:

$$\langle I \rangle = \frac{e^2}{h} |eV| \int \rho(T) T dT \quad (3)$$

$$S = \frac{2e^2}{h} |eV| \int \rho(T) T (1 - T) dT = 2eF \langle I \rangle, \quad (4)$$

where $F \leq 1$ is the Fano factor. For a conventional tunnel junction transmissions are small and $\rho(T)$ is substantial

only for $T \ll 1$. We then may disregard the $\sim T^2$ term in the integrand of Eq. (4) and classical shot noise corresponding to $F \rightarrow 1$ is recovered. Clearly, a suppression of the shot noise that would correspond to a Fano factor significantly smaller than unity requires that $\rho(T)$ is significant at transmissions close to unity. Indeed, below we find such highly transmitting states in MTJs with sufficiently thin barriers.

Previous theoretical treatments of the statistics of quantum transport have been limited to simple models. While these can be sufficiently accurate for, *e.g.*, structures defined on a two-dimensional electron gas, the details of the electronic structure are essential to understand (nearly) ballistic MTJs [11, 12, 22]. This Letter reports the results of material-specific first principles calculations of the statistics of transport in Fe|MgO|Fe magnetic tunnel junctions as a function of magnetic configuration, voltage bias, and interface morphology and compare theory with experiments by Arakawa *et al.* [21], in particular the suppression of the Fano factor for the parallel configuration.

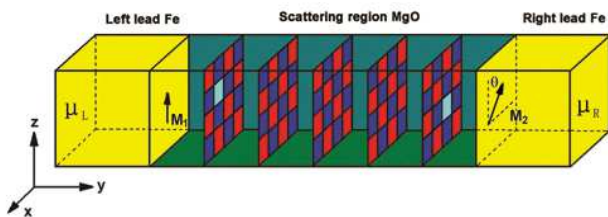


FIG. 1: (Color online) Schematic diagram of a Fe|MgO|Fe(001) junction containing 5 MgO monolayers. The magnetization \mathbf{M}_1 of the left lead coincides with the z -axis; the magnetization \mathbf{M}_2 of the right lead lies in the xz -plane with angle θ . The red and blue grids in the scattering region denote the O and Mg atoms, respectively. We allow for interfacial disorder (oxygen vacancies, cyan grid) at the Fe|MgO interfaces. The applied bias $eV = \mu_R - \mu_L$, where μ_R and μ_L are the chemical potentials of the right and left leads, respectively.

We consider an MTJ consisting of a MgO barrier and two semi-infinite iron leads as shown in Fig. 1. The electric current flows along the (001) crystal growth direction. We incorporate the small lattice mismatch between the leads and the barrier by a 3% compression of the MgO lattice constant. The self-consistent calculations are carried out with the tight-binding linear muffin-tin orbital (TB-LMTO) [23] surface Green function method [24]. Disorder is treated using the layer CPA (coherent potential approximation) [25]. The atomic sphere (AS) potentials serve as input to the second step, in which the transmission matrix is calculated using a TB-LMTO implementation [26]. Disorder is modeled by large lateral supercells, distributing the self-consistently calculated CPA-AS potentials randomly layer-for-layer in the

appropriate concentrations in as many configurations as necessary. Depending on the defect concentration, most of our results are based on lateral supercells containing 72 (two times 6×6) or 128 (two times 8×8) Fe atoms per monolayer.

$\text{TMR} \equiv R(AP)/R(P) - 1$, where $R(AP)$ [$R(P)$] is the electric resistance for the antiparallel (AP) [parallel (P)] configuration of the lead magnetizations. For 5 MgO monolayers (L) at low bias $\text{TMR} = 3580\%$ for specular interfaces, which decreases drastically to 250% when 5.56% oxygen vacancies (OV, the energetically most favorable defect) are introduced at both interfaces. The TMR for the ideal junction is consistent with published calculations [11], while that for disordered junctions is of the same order of magnitude as found in experiments [5].

Based on the calculated scattering matrix, we compute the Fano factor for various junction parameters. The results are shown in Table I together with the TMR. For thick barriers, the Fano factors are very close to unity, implying full Poisson noise as expected. As the barrier gets thinner, the Fano factor of the parallel configuration is increasingly suppressed. For a 5 MgO layers junction with 5.56% interfacial disorder, the Fano factor is $F_P = 0.87(4)$ and $F_{AP} = 0.98(1)$ for both configuration, close to the experimental values $F_P = 0.91(2)$ and $F_{AP} = 0.98(1)$ for the same thickness [21]. We can identify the majority (\uparrow) and minority (\downarrow) spin contributions to be $F_P^\uparrow = 0.96$ and $F_P^\downarrow = 0.72$, where $F_P^{\uparrow(\downarrow)} \equiv S_P^{\uparrow(\downarrow)} / (2e\langle I_P^{\uparrow(\downarrow)} \rangle)$.

In order to trace the origin of the shot noise suppression, we plot the distribution functions of the transmission matrix eigenvalues $\rho_{P/AP}(T)$ in Fig. 2 involving 7×10^6 eigenvalues over the whole Brillouin zone. For P, we identify a few high values of T_n , which according to Eqs. (3,4) affect shot noise S more strongly than conductance G : 0.3% of the eigenvalues are larger than 0.05 but contribute about 39% to G but 89% to the integrand proportional to T^2 in Eq. (4), which suppresses S . The integrands proportional to T and T^2 are shown for each eigenvalue interval in the histograms of Fig. 2. The dashed bars indicate a larger statistical error caused by the small number of eigenvalues at high T_n . For AP, only very few T_n fall into the region between 0.05 and 0.1, the rest (99.95%) are all less than 0.05.

In Table I we can see that interfacial defects are necessary to explain the observed shot noise suppression [21]. The OV concentration-dependent Fano factor for the 5MgO junction can be found in Table II. The statistics of our supercell calculation is found to be good by comparison with a Green function formalism in which impurity scattering is handled by the CPA [27]. Furthermore, even though an OV concentration around 5% suppresses the Fano factor, a further increase leads to a dramatical recovery of the full shot noise. The full shot noise observed in earlier experiments[19, 20] is therefore

TABLE I: Barrier thickness dependence of the Fano factor in Fe| n MgO|Fe MTJs for the parallel (P) and antiparallel (AP) configuration. The results in square brackets are obtained for disordered junctions with 5.56% oxygen vacancies at the interfaces, where the error bar is given in round brackets.

Fano factor	3MgO	4MgO	5MgO	7MgO
P	0.64[0.65(2)]	0.91[0.69(4)]	0.97[0.87(4)]	1.00[0.99(1)]
AP	0.94[0.77(2)]	1.00[0.94(1)]	1.00[0.98(1)]	1.00[0.99(1)]
TMR	1320%[165%]	2400%[288%]	3580%[250%]	5600%[107%]

TABLE II: OV concentration dependence of the Fano factor in 5MgO MTJs for P and AP configurations. The impurity concentrations are obtained by different numbers of OVs at the interfaces per lateral unit cell. 2 OVs in the 6×6 supercell correspond to 5.56%, 3 or 4 OVs in an 8×8 supercell correspond to 4.69% and 6.25% respectively. The conductances are given in units of $10^{-5} e^2/h$ per Fe atomic interfacial area, where the statistical error bar is given in round brackets. The conductances in square brackets are obtained by the Green function method [27] as a check of the statistics of the supercell method.

Concentration	P			AP	
	G(maj)	G(min)	Fano factor	G	Fano factor
0	68.00[68.50]	3.47[3.51]	0.97	1.95[1.95]	1.00
4.69%	89(3)[94.5]	41(7)[33.6]	0.85(3)	35(3)[32.8]	0.98(1)
5.56%	80(4)[91.0]	44(10)[29.2]	0.87(4)	36(4)[37.5]	0.98(1)
6.25%	79(3)[85.5]	25(4)[26.9]	0.95(2)	38(3)[41.0]	0.98(1)

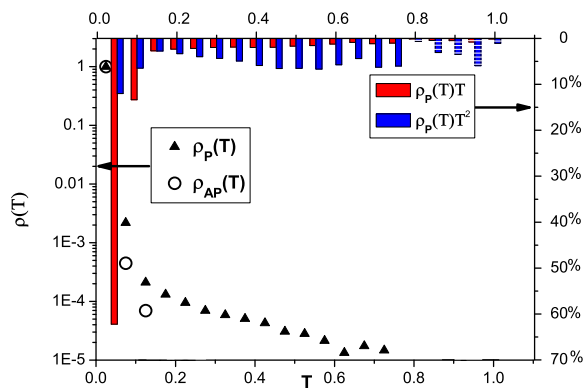


FIG. 2: Distribution of the transmission matrix eigenvalues $\rho(T)$. The open circles are obtained for the AP configuration, for which 99.95% of eigenvalues are $T_n < 0.05$. Solid triangles represent results for the P configuration. While most eigenvalues are still less than 0.05, the few high values prove the presence of resonant tunneling states. The red and blue histograms indicate the contribution of the integrands T and T^2 to each eigenvalue interval (for P). Dashed bars indicated increased statistical error due to the small number of T_n 's approaching unity.

consistent with higher disorder.

In order to understand the sensitivity to the OVs, we plot the energy dependence of the conductance of 5MgO MTJs with different OVs concentrations in Fig. 3. In ballistic junctions the minority spin conductance for P and the AP conductance are strongly suppressed. Below the Fermi energy high transmissions are observed,

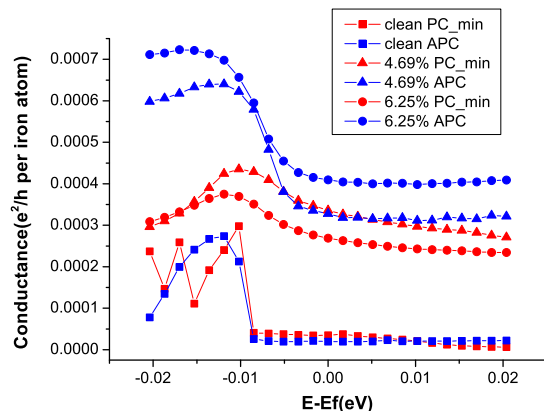


FIG. 3: Energy-dependent conductance for P (minority spin) and AP configuration of a 5MgO MTJ for different impurity concentrations. Filled squares represent the ballistic junction, triangles 4.69% OV disorder, and circles 6.25% OV disorder. Red symbols stand for the minority spin conductance in the P and blue ones for the conductance in the AP configuration.

however. For P these are caused by the overlap between interface states on both sides of the barrier. For AP, the interface states exist only on one side of the barrier, but since their symmetry is not orthogonal to the Δ_1 states in the barrier and the majority spin states on the another side, the conductance is still high. Small amounts of OVs broaden and shift highly transmitting resonant channels toward the Fermi energy, thereby suppressing F_P (and the TMR). However, a further increase of the disorder destroys the resonant channels thereby recovering the full shot noise. The AP peak disappears and

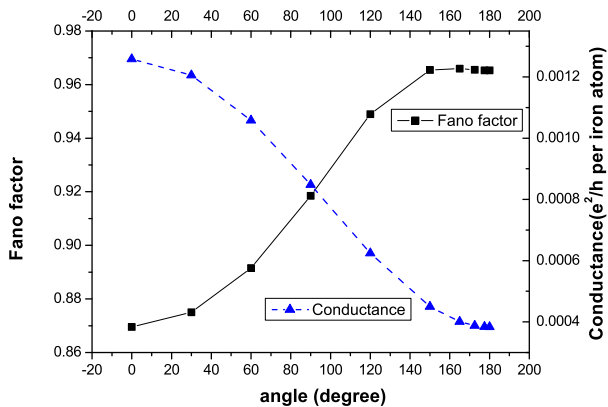


FIG. 4: Angular-dependent Fano factor (triangles) and conductance (squares, per Fe atom at the interface) of 5MgO MTJs with 5.56% OV disorder at the interfaces. When θ changes from P to AP, the conductance decreases monotonously and Fano factor increases.

becomes a step structure near the Fermi energy.

A 5% OV concentration appears to be close to the experiment [21], since it explains both Fano factors and the TMR. Further information may be gained by the θ -dependence of the Fano factor in Fig. 4 for 5MgO junctions with 5.56% OVs. $F(\theta)$ increases when moving from P to AP which can be understood by the arguments above.

An important issue of the current-induced spin transfer torque (STT) in MTJs is its bias dependence. Recent experiments [28] discovered a nonlinear increase of the STT and current at an applied bias of 0.2 V. This value is far below the MgO band gap as calculated in the local density approximation (LDA) [22]. Since the LDA strongly underestimates band gaps, the observed threshold must have a different origin. A recent first principles analysis of the STT in Fe|MgO|Fe junctions explained the threshold in terms of resonant transmission channels in the AP configuration [29]. This hypothesis can be tested by the bias dependence of the shot noise. At finite bias V , the zero temperature current and shot noise read [1]

$$I(V) = \frac{e^2}{h} \int^{eV} \left[\int \rho(T, E) T dT \right] dE \quad (5)$$

$$S(V) = \frac{2e}{h} \int^{eV} \left[\int \rho(T, E) T (1 - T) dT \right] dE \quad (6)$$

Fig. 5 shows the integrated current and Fano factor as a function of applied bias for an Fe(\uparrow)|5MgO|Fe(\downarrow) junction. The Fano factor is unity for low bias but suddenly decreases with increasing bias at the threshold of the nonlinear current characteristic, which for a clean junction is at about 0.8 V, consistent with the threshold bias in the STT. Small amounts of oxygen vacancies in MgO can lower this threshold bias to become closer to the experi-

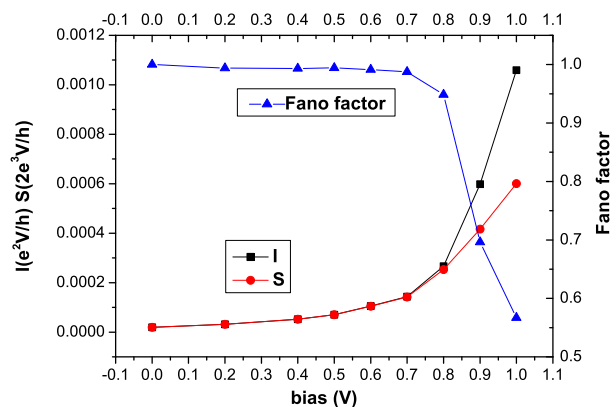


FIG. 5: Bias voltage-dependent Fano factor of an antiparallel 5MgO MTJ. I and S stand for current (per Fe atom at the interface) and shot noise integrated over the bias window, respectively.

mental value [29].

In conclusion, we compute sub-Poissonian shot noise for magnetic junctions with thin MgO barriers from first principles in good agreement with experiments. We interpret these results as strong evidence for resonant tunneling states weakly broadened by disorder scattering. While it was known that MgO based tunneling junctions can be grown with high crystalline quality, we believe that the implied wave functions coherence over the tunneling barrier is an important piece of information that lends credibility to the prediction of large thermal spin transfer torques [30]. This additional evidence of the superior electronic properties of MgO junctions should have ramifications for the application of this materials to other than ferromagnetic systems.

We gratefully acknowledge financial support from National Basic Research Program of China under the grant No. 2011CB921803, 2012CB921304, NSF-China, the Dutch FOM Foundation, DFG Priority Program ‘‘Spin-Cat’’, and EU-ICT-7 contract no. 257159 MACALO. We thank the Authors of Ref. 21 for valuable discussions concerning their experimental results.

-
- [1] Ya.M. Blanter and M. Büttiker, *Physics Reports* **336**, 1(2000).
 - [2] *Quantum Noise in Mesoscopic Physics*, edited by Yu. V. Nazarov (Kluwer, Dordrecht, 2003).
 - [3] W. Schottky, *Ann. Phys. (Leipzig)* **57**, 541 (1918) .
 - [4] C.W.J. Beenakker and C. Schönberger, *Physics Today*, May 2003, p. 37.
 - [5] S. Yuasa, T. Nagahama, A. Fukushima, Y. Suzuki, and K. Ando, *Nature Mat.* **3**, 868 (2004).
 - [6] S. S. P. Parkin, C. Kaiser, A. Panchula, P. M. Rice, B. Hughes, M. Samant, and S.-H. Yang, *Nat. Mat.* **3**, 862

- (2004).
- [7] S. C. Oh, S. Y. Park, A. Manchon, M. Chshiev, J. H. Han H.-W. Lee, J.-E. Lee, K.-T. Nam, Y. Jo, Y.-C. Kong, B. Dieny, K.-J. Lee, *Nat. Phys.* **5**, 898 (2009).
- [8] A. M. Deac, A. Fukushima, H. Kubota, H. Maehara, Y. Suzuki, S. Yuasa, Y. Nagamine, K. Tsunekawa, D. D. Djayaprawira, and N. Watanabe, *Nat. Phys.* **4**, 803 (2008).
- [9] M. H. Jung, S. Park, C. -Y. You, S. Yuasa, *Phys. Rev. B* **81**, 134419 (2010).
- [10] R. Matsumoto, A. Fukushima, K. Yakushiji, S. Yakata, T. Nagahama, H. Kubota, T. Katayama, Y. Suzuki, K. Ando, S. Yuasa, B. Georges, V. Cros, J. Grollier, and A. Fert, *Phys. Rev. B* **80**, 174405 (2009).
- [11] W. H. Butler, X.-G. Zhang, and T. C. Schulthess, and J. M. MacLaren *Phys. Rev. B* **63**, 054416 (2001)
- [12] J. Mathon, and A. Umerski, *Phys. Rev. B* **63**, 220403 (2001).
- [13] J. M. De Teresa, A. Barthél my, A. Fert, J. P. Contour, F. Montaigne, and P. Seneor, *Science* **286**, 507 (1999).
- [14] G. X. Miao Y. J. Park, J. S. Moodera, M. Seibt, G. Eilers, and M. M nzenberg, *Phys. Rev. Lett.* **100**, 246803 (2008).
- [15] P. G. Mather, J. C. Read, and R. A. Buhrman, *Phys. Rev. B* **73**, 205412 (2006).
- [16] P. X. Xu, V. M. Karpan, K. Xia, M. Zwierzycki, I. Marushchenko, and P. J. Kelly, *Phys. Rev. B* **73**, 180402(R) (2006).
- [17] J. P. Velev, K. D. Belashchenko, S. S. Jaswal, and E.Y. Tsybmal, *Appl. Phys. Lett.* **90**, 072502 (2007).
- [18] Y. Ke, K. Xia, and H. Guo, *Phys. Rev. Lett.* **105**, 236801 (2010).
- [19] R. Guerrero, D. Herranz, F.G. Aliev, F. Greullet, C. Tiusan, M. Hehn, and F. Montaigne, *Appl. Phys. Lett.* **91**, 132504(2007)
- [20] K. Sekiguchi, T. Arakawa, Y. Yamauchi, K. Chida, M. Yamada, H. Takahashi, D. Chiba, K. Kobayashi, and T. Ono, *Appl. Phys. Lett.* **96**, 252504 (2010)
- [21] T. Arakawa, K. Sekiguchi, S. Nakamura, K. Chida, Y. Nishihara, D. Chiba, K. Kobayashi, A. Fukushima, S. Yuasa, and T. Ono, *Appl. Phys. Lett.* **98**, 202103 (2011).
- [22] C. Heiliger, and M. D. Stiles, *Phys. Rev. Lett.* **100**, 186805 (2008).
- [23] O. K. Andersen, Z. Pawlowska, and O. Jepsen, *Phys. Rev. B* **34**, 5253 (1986)
- [24] I. Turek, V. Drchal, J. Kudrnovsky, M. Sob, and P. Weinberger, *Electronic Structure of Disordered Alloys, Surfaces and Interfaces* (Kluwer, Boston, 1997).
- [25] P. Soven, *Phys. Rev.* **156**, 809 (1967)
- [26] K. Xia, M. Zwierzycki, M. Talanana, P. J. Kelly, and G. E. W. Bauer, *Phys. Rev. B* **73**, 064420 (2006).
- [27] Y. Ke, K. Xia, and H. Guo, *Phys. Rev. Lett.* **100**, 166805 (2008).
- [28] C. Wang, Y.-T. Cui, J. A. Katine, R. A. Buhrman, and D. C. Ralph, *Nature Phys.* **7**, 496 (2011)
- [29] Xingtao Jia, Ke Xia, Youqi Ke, Hong Guo, *Phys. Rev. B* **84**, 014401 (2011).
- [30] X. Jia, Ke Xia, and G.E.W. Bauer, *Phys. Rev. Lett.* **107**, 176603 (2011).